Development of tissue factor-targeted liposomes for effective drug delivery to stroma-rich tumors

Development of tissue factor-targeted liposomes for effective drug delivery to stroma-rich tumors

Kosuke Shimizu[a,b,*], Yoshihito Takeuchi[b], Kazuma Otsuka[b], Tomoya Mori[b], Yudai Narita[a,b], Shohei Takasugi[b], Yasuhiro Magata[a], Yasuhiro Matsumura[c], Naoto Oku[b,d,**]

[a]Department of Molecular Imaging, Institute of Medical Photonics Research, Preeminent Medical Photonics Education & Research Center, Hamamatsu University School of Medicine, 1-20-1 Handayama, Higashi-ku, Hamamatsu City, Shizuoka 431-3192, Japan

[b]Department of Medical Biochemistry, School of Pharmaceutical Sciences, University of Shizuoka, 52-1 Yada, Suruga-ku, Shizuoka City, Shizuoka 422-8526, Japan

[c]Division of Developmental Therapeutics, Exploratory Oncology Research & Clinical Trial Center, National Cancer Center, 6-5-1 Kashiwanoha, Kashiwa City, Chiba 277-8577, Japan

[d]Laboratory of Bioanalytical Chemistry, Faculty of Pharma-Science, Teikyo University, 2-11-1 Kaga, Itabashi-ku, Tokyo 173-8605, Japan

*Corresponding author:
Kosuke Shimizu, Ph.D.
Department of Molecular Imaging, Institute for Medical Photonics Research, Preeminent Medical Photonics Education & Research Center, Hamamatsu University School of Medicine
1-20-1 Handayama, Higashi-ku, Hamamatsu City, Shizuoka 431-3192, Japan
kshimizu@hama-med.ac.jp

** Corresponding author:
Naoto Oku, Ph.D.
Laboratory of Bioanalytical Chemistry, Faculty of Pharma-Science, Teikyo University
2-11-1 Kaga, Itabashi-ku, Tokyo 173-8605, Japan
noku@pharm.teikyo-u.ac.jp

Keywords: Antibody; liposome; pancreatic tumor; targeting; tissue factor; tumor stroma

Abstract

Tissue factor (TF), which is well known as a trigger molecule of extrinsic coagulation, is found in not only tumor cells but also in stromal cells in tumor tissues. Thus, TF is a candidate molecule to potentially enable targeting of both tumor cells and stromal cells for anti-cancer drug delivery. Herein, we prepared liposomes conjugated with the Fab' fragment of anti-TF antibody (TF Ab-Lip) and evaluated the capability for drug delivery to stroma-rich tumors for realizing a whole tumor tissue-targetable strategy. When the targetability of TF Ab-Lip to TF-expressing KLN205 squamous tumor cells and NIH3T3 fibroblast cells were examined, TF Ab-Lip was significantly taken up into both cells compared with non-targeted liposomes. Corresponding to this result, doxorubicin-encapsulated TF Ab-Lip (TF Ab-LipDOX) showed potent cytotoxicity against KLN205 cells. *In vivo* experiments using KLN205 solid tumor-bearing mice indicated that TF Ab-Lip became highly accumulated and distributed widely in not only the tumor cell region but also in the stromal one in the tumor. Treatment with TF Ab-LipDOX significantly suppressed the growth of KLN205 solid tumors. Furthermore, TF Ab-Lip targetable both mouse and human TF (mhTF Ab-Lip) became distributed throughout stroma-rich human pancreatic BxPC3 tumors and the treatment of the BxPC3 tumor-bearing mice with mhTF Ab-LipDOX showed highest tumor-suppressive effect. These data suggest that TF Ab-Lip could achieve effective accumulation for stroma-rich tumor treatment.

1. Introduction

The importance of the tumor microenvironment in tumor malignancy is attracting much attention, and the tumor stroma is one of the factors composing this microenvironment. Theise *et al.* recently demonstrated that stroma functions not only in human body homeostasis but also in tumor metastasis and advocated that the stroma is an "organ" in the body [1]. In fact, stromal cells are widely distributed in certain malignant tumor tissues such as pancreatic tumors and gliomas; and they promote tumor cell growth by making contact with each other and secreting certain cytokines such as transforming growth factor (TGF)-β [2, 3]. Furthermore, the tumor stroma is involved in drug resistance by working just like a defense wall against the blood flow components and circulating drugs and thus preventing drug penetration into the internal area of tumor tissues [4]. Thus, the anti-tumor approach with emphasis on the tumor stroma is now being considered [5].

On the other hand, since the relationship between tumor development and blood coagulation has been advocated [6] and clinical data indicate that cancer patients frequently suffer from thrombosis [7], the expression of blood-coagulation factors in tumor tissue is now a topic for discussion [8, 9]. Among these factors, tissue factor (TF), also referred to as thromboplastin or blood coagulation factor III, is a 47-kDa transmembrane glycoprotein that is known to work as an initiator in extrinsic coagulation protease cascades: TF is expressed in the extravascular stroma in normal tissues, where it can avoid contact with the blood circulation under physiological conditions. However, when external physical damage to the tissues occurs, TF makes contact with other blood coagulation factors such as factor VII, thus initiating the blood coagulation process. Besides, enhanced expression of TF has also been found in various kinds of tumors; and the expression is notably observed throughout the tumor tissue; i.e., TF is expressed in not only angiogenic vessels and stromal cells but also in tumor cells in the tumor tissues [10, 11]. Therefore, TF would seem to be a suitable target molecule for effective drug delivery to stroma-rich tumors.

The liposome is a highly safe and valuable drug nanocarrier and is used for effective drug delivery to disease sites and improving the pharmaceutical problems of ingredients. In fact, liposomal formulations encapsulating anti-cancer drugs have already been used for cancer chemotherapy all over the world; and therapeutic advantages such as shrinkage of solid tumors and reduced side effect have been obtained [12]. However, the application of liposomal agents has been limited in some kinds of tumors; and insufficient therapeutic efficacy toward stroma-rich tumors such as pancreatic tumors has been noted. Therefore, to overcome the weak points of liposomal drugs, a new liposome delivery approach avoiding the defense by tumor stroma must

be proposed. Herein, to improve the therapeutic efficacy of liposomal drug toward stroma-rich tumors, we prepared liposomes conjugated with the Fab' fragment of anti-TF antibody, which enabled targeting not only TF-expressing tumor cells but also TF-expressing stromal cells. Using such liposomes, we evaluated the capability for whole tumor tissue-targeting delivery.

2. Materials and Methods

2.1. Materials

Anti-mouse TF rat monoclonal IgG_{2a} antibody was produced and purified as previously reported, and clone 1157 was used in each experiment. Mouse recombinant tissue factor was purchased from R&D Systems. Distearolyphosphatidylcholine (DSPC), cholesterol (Cho), and *N*-(Carbonyl-methoxypolyethyleneglycol 2000)-1,2-distearoyl-*sn*-glycero-3-phosphoethanolamine (DSPE-MPEG) were obtained from Nippon Fine Chemical Co., Ltd. (Takasago, Hyogo, Japan). *N*-[(3-Maleimide-1-oxopropyl)aminopropyl polyethyleneglycol 2000-carbamyl] distearoylphosphatidyl-ethanolamine (SUNBRIGHT DSPE-020-MA, DSPE-PEG-Mal) was purchased from NOF Corporation (Tokyo, Japan). 1,1'-Dioctadecyl-3,3,3',3'-tetramethylindocarbocyanine perchlorate ($DiIC_{18}$), 3,3'-dioctadecyloxacarbocyanine perchlorate ($DiOC_{18}$), and 1,1'-dioctadecyltetramethyl indotricarbocyanine iodide (DiR) were procured from Life Technologies Japan (Tokyo, Japan).

2.2. Cell culture

Mouse squamous tumor cell line KLN205, mouse melanoma cell line B16F10 (B16), mouse colon carcinoma cell line Colon26 NL-17 (Colon26), mouse fibroblast cell line NIH3T3, and mouse endothelial cell line 2H-11 were cultured in D-MEM (high glucose) medium (Wako Pure Chemical Industries) supplemented with 10% heat-inactivated FBS (Hyclone, GE Healthcare Japan), 100 μg/mL streptomycin (MP Biomedicals), and 100 units/mL penicillin (MP Biomedicals) at 37°C in a humidified atmosphere with 5% CO_2. Human pancreatic adenocarcinoma cell line BxPC3 and human pancreatic cancer cell line Suit-2 were also cultured in RPMI-1640 medium (Wako Pure Chemical Industries) containing 10% FBS.

2.3. Animals

DBA/2 male mice and BALB/c nu/nu male mice were purchased from Japan SLC (Shizuoka, Japan). All animal experiments were performed at the University of Shizuoka and approved by the Animal and Ethics Committee of the University of Shizuoka. The animals were

cared for according to the Animal Facility Guidelines of the University of Shizuoka. For preparation of solid tumor-bearing mice, KLN205 cells in D-MEM medium were subcutaneously implanted (5 x 10^6 cells/0.2 mL/mouse) into DBA/2 male mice; and when the tumor size reached about 1 cm in diameter, the tumor-bearing mice were used for each experiment. To prepare human pancreatic tumor-bearing mice, we implanted BxPC3 cells (5 x 10^6 cells / 0.2 mL / mouse) subcutaneously into BALB/c nu/nu male mice.

2.4. Western blotting

Cultured cells were lysed for 30 min at 4°C with 1% Triton X-100/Tris buffer (pH 7.4) containing protease inhibitors (10 mM PMSF, 200 μg/mL Aprotinin, 200 μg/mL Pepstatin-A, and 200 μg/mL Leupeptin); and the amount of protein was determined by use of a BCA protein assay kit (PIERCE). The protein samples were subjected to SDS-PAGE, transferred to a PVDF membrane (Millipore), and blocked with 3% BSA in TTBS (0.9% NaCl, 0.1% Tween20, 20 mM Tris-HCl; pH 7.4). The primary antibodies used were rat anti-mouse TF monoclonal antibody, rat anti-human TF monoclonal antibody, and rabbit anti-β-actin polyclonal antibody (SIGMA-Aldrich). Goat anti-rat IgG horseradish peroxidase (HRP)-conjugated antibody or donkey anti-rabbit IgG HRP-conjugated antibody (Thermo Fisher Scientific) was used as the secondary antibodies. The PVDF membrane was developed with ECL prime reagent (GE Healthcare) and scanned with a LAS-3000UVmini (Fujifilm). Solid tumor samples were lysed with a tissue-protein extraction reagent (Thermo Fisher Scientific). and the expression of TF was determined by Western blotting as described above.

2.5. Immunostaining

KLN205 solid tumors were harvested from the tumor-bearing mice, embedded in optical cutting temperature (O.C.T.) compound, and frozen at -80°C with dry ice. Ten-micrometer frozen sections were prepared with a HM505E cryostatic microtome (MICROM) and transferred to MAS-coated glass slides (Matsunami Glass Ind., Ltd.). Then, the tumor sections were fixed with 4% paraformaldehyde-PBS and thereafter blocked with 3% BSA-PBS at room temperature. For TF staining, sections were probed with anti-mouse TF monoclonal rat antibody (clone 1157) as the primary antibody followed by Alexa Fluor 488 anti-rat IgG antibody as the secondary antibody (Thermo Fisher Scientific); and for α-SMA staining, with Cy3-conjugated anti-α-SMA antibody (SIGMA-Aldrich). In the case of EpCAM staining as a marker of tumor cells, sections were incubated with anti-EpCAM rabbit antibody (Abcam) as the primary antibody followed by

Alexa Fluor 488 anti-rabbit IgG antibody (Thermo Fisher Scientific) as the secondary antibody. After having been washed with PBS, the sections were incubated with DAPI for nuclear staining. Finally, the sections were mounted with PermaFluor™ Aqueous Mounting Medium (Thermo Fisher Scientific). The fluorescence was observed by use of a confocal laser-scanning microscope (LSM510META, Carl Zeiss).

2.6. Preparation of Fab' fragment of anti-TF monoclonal IgG antibody

Whole anti-mouse TF rat IgG_{2a} monoclonal antibody in 100 mM sodium citrate buffer (pH 3.5) was mixed with pepsin (4 w/w%; from porcine gastric mucosa, Sigma-Aldrich) and incubated at 37˚C for 3 h to eliminate the Fc region of the IgG antibody. After the reaction was stopped by the addition of 3 M Tris HCl buffer (pH 8.0), the generated $F(ab')_2$ fragment was washed with 100 mM phosphate buffer (pH 6.8) and concentrated with an Amicon® Ultra-15 (30,000 NMWL, MILLIPORE). Then, the $F(ab')_2$ was reduced by reacting it with 2.5 mM cysteamine hydrochloride (Wako) at 37˚C for 90 min, after which the reaction solution was purified by gel-filtration chromatography (φ1 cm x 45 cm, Ultrogel AcA54, PALL Life Sciences) to obtain the Fab' fragment. The Fab' fraction was determined by measuring the absorbance at 280 nm and concentrated by ultrafiltration with an Amicon® Ultra-4 (30,000 NMWL, MILLIPORE).

2.7. Preparation of anti-TF antibody-conjugated liposomes

DSPC and cholesterol (2 : 1 as a molar ratio) were mixed in chloroform solution and lyophilized with *t*-butanol. Then, the lipids were hydrated with HEPES-buffered solution (pH 7.4) heated up to 60˚C and subsequently frozen in liquid nitrogen and thawed repeatedly for 3 cycles. After sonication for 10 min, the liposomes were passed through 100-nm pore-size polycarbonate membrane filters (Nuclepore) with a Lipex™ extruder (Northern Lipids Inc.) at 65˚C. For radiolabeling of liposomes, [^{3}H]cholesteryl hexadecyl ether (PerkinElmer Japan Co., Ltd.) was mixed in the lipid/chloroform solution before the lyophilization. For fluorescence labeling of liposomes, $DiIC_{18}$, $DiOC_{18}$ or DiR was added in the same manner.

For conjugation of anti-TF antibody to the liposomal surface, DSPE-PEG-Mal was used as a linker molecule. DSPE-PEG-Mal was mixed with a solution of plain liposomes (DSPC / DSPE-PEG-Mal = 1 / 0.05 as a molar ratio), and the mixture was then incubated at 65˚C for 15 min to obtain PEG-Mal-conjugated liposomes. Then, the Fab' fragment of anti-mouse TF monoclonal IgG antibody was added to the PEG-Mal-conjugated liposomes; and the reaction for

the coupling of the maleimide group of the lipid derivative with a thiol group of the Fab' fragment was carried out overnight at 37˚C. After the coupling reaction was stopped by incubation with 1 mM 2-mercaptoethanol for 30 min at 37˚C, the anti-mouse TF antibody-conjugated liposomes (TF Ab-Lip or mTF Ab-Lip) were purified by 3 cycles of ultracentrifugation (550,000 x g, 15 min, 4˚C; CS120GXL, Hitachi Co., Ltd.). The amount of the Fab' fragment was measured by HPLC. Particle size and ζ-potential of liposomes were determined with a ZetaSizer Nano ZS (Malvern Instruments Ltd).

To prepare PEG-modified liposomes (PEG-Lip), we used DSPE-MPEG instead of DSPE-PEG-Mal. For control antibody-conjugated liposomes (Cont Ab-Lip), the Fab' fragment of control rat IgG antibody (Equitech-Bio Inc.) was used instead of anti-mouse TF antibody; and the modification of the liposomes was carried out in the same manner. For the preparation of anti-human TF antibody-conjugated liposomes (hTF Ab-Lip), the Fab' fragment of anti-human TF antibody was prepared and then conjugated to the liposomes. Liposomes conjugated with both anti-mouse and anti-human TF (mhTF) were also prepared as described above.

For doxorubicin (DOX) encapsulation into liposomes, a remote-loading method using ammonium sulfate was applied. In brief, a thin lipid film was hydrated with 250 mM ammonium sulfate solution; and after sizing of the liposomes, the liposomes were dialyzed against water overnight to generate a pH gradient. After ultracentrifugation of the liposomes, the liposomes were suspended with 20 mM HEPES buffer (pH 7.4). Then, DOX (2 mg/mL) solution was added to the liposome solution; and incubation was carried out at 65˚C for 1 h. Unencapsulated DOX was removed by ultracentrifugation, and the pelleted liposomes were resuspended in 20 mM HEPES buffer (pH 7.4). Conjugation of anti-TF antibody to the liposomes was then done as described above.

2.8. Liposome association assay

KLN205 cells (2.0 x 10^4 cells/well), B16F10 cells (1.5 x 10^4 cells/well), NIH3T3 cells (1.5 x 10^4 cells/well) or 2H-11 (1.5 x 10^4 cells/well) cells were seeded onto the wells of a poly-L-lysine-coated 96-well plate and incubated at 37˚C overnight. After removal of the medium, the cells were incubated in fresh medium containing $DiIC_{18}$-labeled PEG-Lip, Cont Ab-Lip or TF Ab-Lip (DSPC concentration of 0.5 mM) for 3 or 24 h. Then, the cells were washed with PBS and lysed with 0.1% SDS/Tris buffer solution (pH 7.4). To determine the association of liposomes with the cells, we measured the fluorescence intensity of DiI (Ex. 549 nm; Em. 592 nm) by using an Infinite M200 microplate reader (Tecan Japan Co., Ltd.). In the case of association with human

tumor cell lines, fluorescently labeled hTF Ab-Lip were incubated with BxPC3 or Suit-2 cells; and the fluorescence was measured in a similar manner.

To observe the uptake of liposomes into TF-expressing tumor cells, we incubated $DiIC_{18}$-labeled PEG-Lip, Cont Ab-Lip or TF Ab-Lip with KLN205 cells for 3 h at 37˚C. After nuclear staining with DAPI, the fluorescence was observed with a confocal laser-scanning microscope (LSM 510 META, Carl Zeiss).

2.9. In vitro cytotoxicity assay

KLN205 cells (1.0×10^4 cells/well) or B16F10 cells (5.0×10^3 cells/well) were seeded onto the wells of a poly-L-lysine-coated 96-well plate and cultured overnight. DOX-encapsulated PEG-modified liposomes (PEG-LipDOX), DOX-encapsulated Cont Ab-Lip (Cont Ab-LipDOX) or TF Ab-LipDOX with DOX doses at 0.1, 0.5, 1, 5, 10 μg/mL were added to the cells; and 12 h later, the cells were washed with PBS. Then, they were cultured in fresh medium without liposomes for 48 h. The viable cells were determined by performing a WST-8 assay: Cell Counting Kit-8 (Dojindo Laboratory) solution was added to the medium and after a 1-h incubation at 37˚C, the absorbance at a wavelength at 450 nm and that of the reference one at 630 nm were measured by an Infinite M200 microplate reader. To determine their cytotoxicity against human pancreatic tumor BxPC2 cells, we incubated PEG-LipDOX, Cont Ab-LipDOX or DOX-encapsulated hTF Ab-Lip (hTF Ab-LipDOX) with the cells and evaluated the suppressive effect on the tumor cell proliferation by performing the WST-8 assay.

2.10. Quantitative analysis of liposome accumulation in solid tumor

[^{3}H]-labeled PEG-Lip, Cont Ab-Lip or TF Ab-Lip (DSPC concentration: 1 mM) were intravenously injected into KLN205 tumor-bearing mice via a tail vein (74 kBq/0.2 mL/mouse). Then, 3 or 24 h later the mice were sacrificed; and the plasma and solid tumor were collected. After the samples had been solubilized with Solvable™ (PerkinElmer Inc.) at 50˚C overnight, the dissolved samples were subsequently mixed with Hionic-Fluor™ (PerkinElmer Inc.). Thereafter, the radioactivity was measured by using a liquid scintillation counter (LSC-7400, Hitachi Aloka Medical, Ltd.). The distribution data were presented as the percentage of injected dose per 100-mg tissue weight. The total weight of plasma was assumed to be 4.38% of the body weight.

2.11. Intratumoral distribution of liposomes

$DiOC_{18}$ or DiR-labeled PEG-Lip, Cont Ab-Lip or TF Ab-Lip were intravenously injected into KLN205 tumor-bearing mice via a tail vein; and after 24 h, their solid tumors were perfused with an excess amount of PBS in order to remove the circulating liposomes in the tumor vessels. The liposomes that had accumulated in the tumor tissue were imaged by use of an *in vivo* fluorescence imaging system (IVIS Lumina, Perkin Elmer). Also, after dissection, frozen tumor sections were prepared; and immunostaining was carried out as described above. The localization of liposomes and stromal cells in the tumor was observed by use of a fluorescence microscope (IX71, Olympus) and an LSM510META confocal laser-scanning microscope.

2.12. Therapeutic experiment

KLN 205 tumor cells (5×10^6 cells) were subcutaneously implanted into DBA/2 male mice (day 0), and TF Ab-LipDOX solutions (0.2 mL) with various DOX dosages (1, 2, or 5 mg/kg/day) were intravenously injected via a tail vein at day 7, 10, 13, and 16 after the tumor implantation. In addition, to compare the tumor-suppressive effect with that of other drug formulations, we injected KLN205 tumor-bearing mice with DOX, PEG-LipDOX, Cont Ab-LipDOX or TF Ab-LipDOX at a DOX dosage of 5 mg/kg/day at days 6, 8, 10, 12, and 14 after tumor implantation. The tumor volume and the body weight changes were monitored daily. The tumor volume was calculated according to the following formula: Tumor volume = $0.4 \times a \times b^2$ (a; largest diameter, b; smallest diameter).

2.13. Human pancreatic tumor targeting experiment

BxPC3 cells (5×10^6 cells) were subcutaneously implanted into BALB/c nu/nu male mice for preparing human pancreatic tumor-bearing mice. For observation of the liposome distribution in the solid tumors, $DiIC_{18}$-labeled PEG-Lip, Cont Ab-Lip, mTF Ab-Lip, hTF Ab-Lip or mhTF Ab-Lip were intravenously injected into the tumor-bearing mice via a tail vein; and after 24 h, the tumor frozen sections were prepared. Then, the sections were stained with Cy3-conjugated anti-α-SMA antibody and DAPI; and intratumoral distribution of the DiI fluorescence was observed with the LSM510META microscope.

To determine the therapeutic effect on human pancreatic tumor, we injected DOX, PEG-LipDOX, mTF Ab-LipDOX, hTF Ab-LipDOX or DOX-encapsulated mhTF Ab-Lip (mhTF Ab-LipDOX) at a dosage of 5 mg/kg/day at days 8, 13, 18, and 23 into BxPC3 tumor-bearing mice after tumor implantation and measured the solid tumor size.

3. Results

3.1. Preparation of stroma-rich mouse tumor model

To select the TF-expressing tumor cells, we first examined the expression of mouse TF in mouse tumor cell lines of squamous KLN205 carcinoma, B16F10 melanoma, Colon26 carcinoma, lung LLC carcinoma, and Meth A fibrosarcoma. The results indicated that the TF expression was higher in both KLN205 and B16F10 cells than that in the other cells (Fig. 1A). Additionally, when the expression of TF in non-tumor cells such as mouse fibroblast NIH3T3 cells and endothelial 2H-11 cells was also examined, the TF expression in the NIH3T3 cells was obviously higher than that in the 2H-11 ones, suggesting that TF expression was enhanced in both tumor and stromal fibroblast cells (Fig. 1A). Next, 2 kinds of tumor-bearing mice in which the TF expression in the tumor cells was either high or low were prepared; and the TF expression in the whole tumor tissue was compared. As the result, TF expression in the KLN205 solid tumor

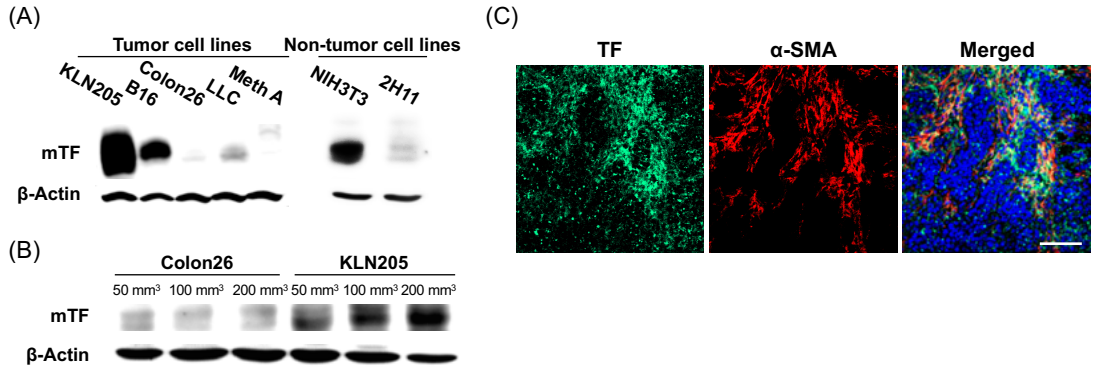

Fig. 1. Preparation of stroma-rich mouse tumor model

(A) TF expression in tumor and non-tumorous cell lines. Mouse KLN205 squamous tumor cells, B16F10 melanoma (B16) cells, Colon26 NL-17 carcinoma (Colon26) cells, Lewis lung carcinoma (LLC) cells, Meth A fibrosarcoma cells, mouse NIH3T3 fibroblast cells, and mouse 2H-11 endothelial cells were cultured; and the expression levels of mouse TF (mTF) and β-actin were examined by Western blotting. (B) TF expression in solid tumors. Colon26 or KLN205 tumor cells were subcutaneously implanted into mice to prepare solid tumor-bearing mice. The amounts of expression of TF and β-actin in the tumors were examined, once their sizes had reached the indicated volumes. (C) Distribution of TF expression in KLN205 solid tumor. Frozen sections of the KLN205 tumor were prepared and immunostained for TF (green), α-smooth muscle actin (α-SMA, red) for stromal staining, and DAPI (blue) for nuclear staining. Scale bar represents 100 μm.

was significantly higher than that in the Colon26 solid tumor; and the expression increased with tumor progression (Fig. 1B). Moreover, the distribution of TF expression in the KLN205 solid tumor was confirmed by immunostaining of both TF and α-SMA, the latter of which was used as a marker of stromal cells in the KLN205 solid tumor. Microscopic observation indicated that TF was widely distributed in the tumor tissue, and the factor was also expressed in many α-SMA-positive cells, suggesting that TF was expressed in not only the tumor cell region but also in the

stromal one in the tumor tissue and indicating that the KLN205 solid tumor is a model of a stroma-rich tumor (Fig. 1C).

3.2. Characterization of TF Ab-Lip and TF Ab-LipDOX

TF Ab-Lip and TF Ab-LipDOX showed similar particle sizes and ζ-potentials in comparison with those of PEG-Lip, PEG-LipDOX, Cont Ab-Lip, and Cont Ab-LipDOX: The average particle sizes of PEG-Lip, PEG-LipDOX, Cont Ab-Lip, Cont Ab-LipDOX, TF Ab-Lip, and TF Ab-LipDOX were 133 nm, 132 nm, 141 nm, 145 nm, 130 nm, and 141 nm, respectively; and their ζ-potentials, -3.0 mV, -2.3 mV, -8.3 mV, -6.2 mV, -8.8 mV, and -7.3 mV, respectively. The DOX encapsulation ratios for PEG-LipDOX, Cont Ab-LipDOX, and TF Ab-LipDOX were 86, 85, and 84%, respectively (Table S1). To evaluate the specific binding of TF Ab-Lip to the target molecule, TF, we performed a liposome binding assay using the Biacore system. The results indicated that only TF Ab-Lip showed a specific association with the TF-immobilized chip, whereas PEG-Lip and Cont Ab-Lip had so such association (Fig. 2A). Furthermore, TF Ab-Lip did not bind to BSA, suggesting that TF Ab-Lip possessed a selective binding potential for the TF molecule.

3.3. TF-mediated uptake of TF Ab-Lip into TF-expressing cells

Next, a liposome association assay using mouse TF-expressing KLN 205 and B16 cells, and low TF-expressing Colon26 cells was carried out: Fluorescently labeled PEG-Lip, Cont Ab-Lip or TF Ab-Lip was incubated with the cells for 3 or 24 h, after which the fluorescence intensity in the cells was quantitatively analyzed. The results indicated that TF Ab-Lip was associated with KLN205 cells in a time-dependent manner and that the association was significantly higher than that observed with PEG-Lip or Cont Ab-Lip (Fig. 2B). A similar result was obtained with TF-expressing B16F10 cells (Fig. S2A). On the other hand, the association of liposomes into Colon26 cells was very low, with the association level being similar among the various types of liposomes (Fig. 2B). When the liposome uptake in the cells was observed by using confocal laser-scanning microscopy, the fluorescence of $DiIC_{18}$-labeled TF Ab-Lip was obviously localized in the cytosol of not only KLN205 cells (Fig. 2C) but also B16F10 cells (Fig. S2B), suggesting that TF-Ab-Lip could target TF-expressing tumor cells and deliver ingredients into them.

Next, to evaluate the targetability of TF Ab-Lip to stromal cells, we performed a liposome association assay using NIH3T3 and 2H-11 cells. The results revealed that TF Ab-Lip were significantly associated with the TF-expressing NIH3T3 cells compared with the association

of PEG-Lip and Cont Ab-Lip and that the association was similar for TF-expressing KLN205 and B16F10 cells (Fig. 2B, C). In contrast, the association of TF Ab-Lip into 2H-11 cells was similar level to those of PEG-Lip and Cont Ab-Lip (Fig. 2B). These results suggest that TF-Ab-Lip could target stromal fibroblast cells due to the high affinity of these liposomes for the TF molecules on the fibroblast cell surface.

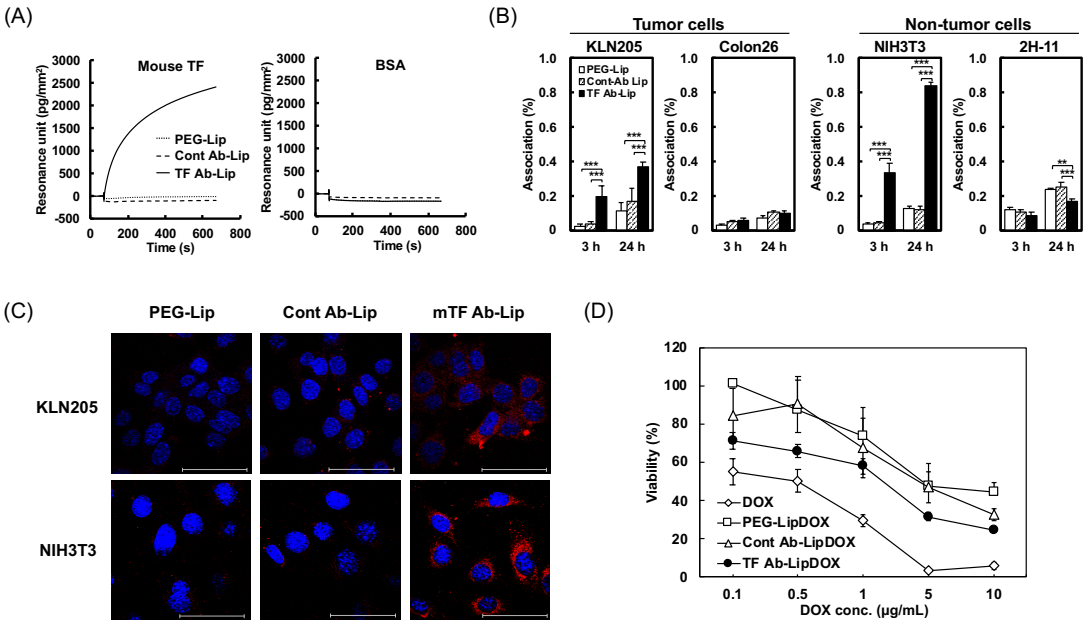

Fig. 2. Targetability of TF Ab-Lip to TF-expressing cells.
(A) Specific binding of TF Ab-Lip to mouse TF. PEG-Lip, Cont Ab-Lip or TF Ab-Lip were reacted with mouse TF- or BSA-immobilized chip, and the interaction was analyzed with the Biacore system. (B) Targeting of TF Ab-Lip to TF-expressing cells. KLN205 tumor, Colon26 tumor, NIH3T3 fibroblast or 2H-11 endothelial cells were incubated with $DiIC_{18}$-labeled PEG-Lip, Cont Ab-Lip or TF Ab-Lip for 3 or 24 h at 37ºC. The percentage of liposome uptake was determined by measuring the fluorescence intensity of DiI in the cells. Significant differences are shown (**, $P < 0.01$; ***, $P < 0.001$, Tukey HSD). (C) Intracellular uptake of TF Ab-Lip into TF-expressing cells. KLN205 or NIH3T3 cells were incubated with $DiIC_{18}$-labeled PEG-Lip, Cont Ab-Lip or TF Ab-Lip (red) for 3 h at 37ºC. After nuclear staining with DAPI (blue), the fluorescence distribution was observed under a confocal laser-scanning microscope. Scale bars represent 50 μm. (D) Cytotoxicity of TF Ab-LipDOX against KLN205 tumor cells. KLN205 cells were incubated for 12 h with DOX, PEG-LipDOX, Cont Ab-LipDOX or TF Ab-LipDOX at DOX doses of 0.1, 0.5, 1, 5, 10 μg/mL; and after having been washed with PBS, the cells were additionally cultured for 48 h. The viable cells were then determined by performing a WST-8 assay.

3.4. Inhibitory effect of TF Ab-LipDOX on proliferation of TF-expressing tumor cells

To demonstrate the potential for drug delivery by TF Ab-Lip to TF-expressing cells, we performed a cytotoxicity assay to examine the anti-proliferative effect of TF Ab-LipDOX against the KLN205 cells. As the result, TF Ab-LipDOX significantly inhibited the proliferation of KLN205 cells compared with non-targeted PEG-LipDOX or Cont Ab-LipDOX (Fig. 2D). The IC_{50} of DOX, PEG-LipDOX, Cont Ab-LipDOX, and TF Ab-LipDOX were 0.2 μg/mL, 5.8 μg/mL,

3.9 μg/mL, and 1.2 μg/mL as DOX concentration, respectively. Similar results were obtained in an experiment using B16F10 cells, where the IC_{50} values for DOX, PEG-LipDOX, Cont Ab-LipDOX, and TF Ab-LipDOX were 0.1 μg/mL, 1.2 μg/mL, 1.1 μg/mL, and 0.3 μg/mL, respectively (Fig. S2C). These results suggested TF Ab-LipDOX to have strong anti-tumor activity and indicated that TF Ab-Lip could be a useful drug carrier to target TF-expressing cells.

3.5. Accumulation of TF Ab-Lip in solid tumors after systemic injection

Next, we prepared radiolabeled PEG-Lip, Cont Ab-Lip, and TF Ab-Lip to examine the biodistribution of these liposomes in KLN205 solid tumor-bearing mice after intravenous injection. The results for 3-h post injection indicated that TF Ab-Lip had obviously accumulated in the solid tumor and that the accumulation was significantly higher than that observed for PEG-Lip or Cont Ab-Lip (Fig. 3A). The retention of TF Ab-Lip in the bloodstream was quite high and similar to that of long-circulating PEG-Lip, whereas that of Cont Ab-Lip was much decreased. The results at 24-h post injection indicated that the accumulation of TF Ab-Lip in the solid tumor increased with time. Additionally, the high accumulation of fluorescently labeled liposomes in the tumor could be imaged by IVIS (Fig. 3B). When the intratumoral distribution of TF Ab-Lip was observed, TF Ab-Lip was found to be located in not only the peripheral region but also the internal area of the KLN205 solid tumor, thus widely distributed in the whole tumor tissue (Fig. 3C). In contrast, the distribution of PEG-Lip and Cont Ab-Lip was limited to only a small part of the tumor tissue (Fig. 3C). Furthermore, to determine the region of the distributed liposomes in detail, we immunostained tumor sections. The results showed that TF Ab-Lip were found not only in the α-SMA-positive stromal region but also in the surrounding tumor cell region in the tumor sections, indicating that TF Ab-Lip was distributed to both tumor cells and stromal cells in the tumor tissue (Fig. 3D). These findings suggest that TF Ab-Lip could actively target both TF-expressing tumor and stromal cells via the binding of anti-TF antibody on the liposomal surface to the TF on these cells, thus suggesting the possibility for effective delivery of encapsulated drugs to stroma-rich tumors by this tumor dual targeting approach.

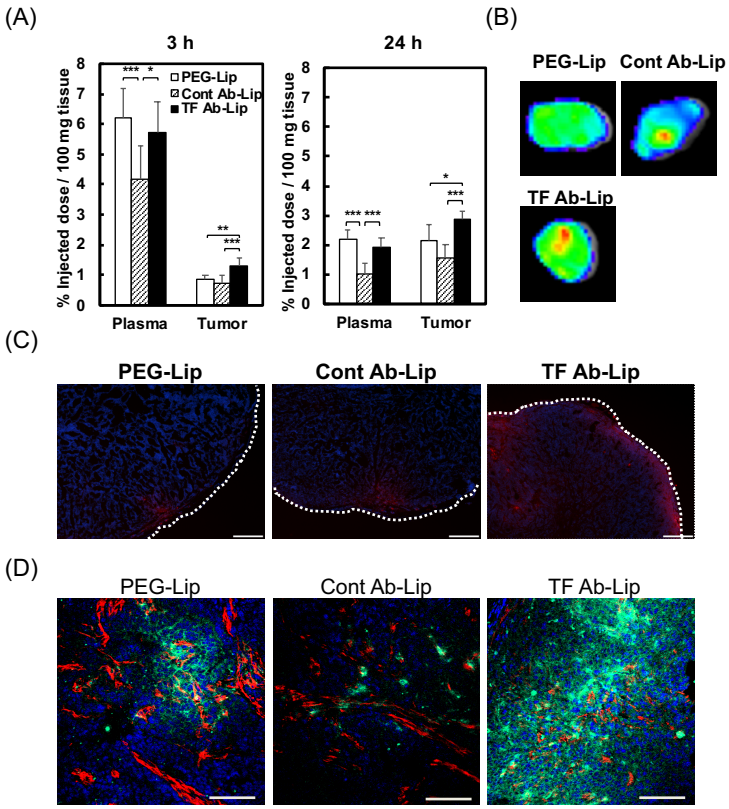

Fig. 3. Stroma-rich tumor targeting by TF Ab-Lip

(A) Quantitative analysis of liposome accumulation in KLN205 solid tumors. Radiolabeled PEG-Lip, Cont Ab-Lip or TF Ab-Lip were intravenously injected into KLN205 solid tumor-bearing mice via a tail vein; and the liposomes were allowed to be distributed for 3 or 24 h. After collecting the plasma and solid tumor, the radioactivity was measured by a liquid scintillation counter. Data are presented as the percentage of the injected dose per 100-mg tissue weight. Significant differences are shown with asterisks (*, $P < 0.05$; **, $P < 0.01$; ***, $P < 0.001$, Tukey HSD). (B, C) Fluorescence imaging of distribution of TF Ab-Lip in KLN205 solid tumors. DiR-labeled PEG-Lip, Cont Ab-Lip or TF Ab-Lip were intravenously injected into KLN205 tumor-bearing mice and allowed to circulate for 24 h. After blood perfusion with PBS, the solid tumors were harvested; and the fluorescence was thereafter scanned with an IVIS system (B). Then, frozen sections were prepared; and nuclei were stained with DAPI (blue). Distribution of DiR fluorescence (red) was observed with a fluorescence microscope (C). White-dotted lines represent the tumor border in the sections. Scale bars represent 500 μm. (D) Intratumoral distribution of TF Ab-Lip in KLN205 solid tumors. $DiOC_{18}$-labeled PEG-Lip, Cont Ab-Lip or TF Ab-Lip were intravenously injected into KLN205 tumor-bearing mice. After 24 h, each solid tumor was harvested and tumor sections prepared. Immunofluorescence staining of α-SMA by using Cy3-conjugated anti-α-SMA antibody (red) was performed to visualize the stromal cells. Nuclei were stained by DAPI (blue). Then, the fluorescence images of the sections were observed. Scale bars represent 100 μm.

3.6. Therapeutic effect of TF Ab-LipDOX on growth of KLN205 solid tumors

To demonstrate the impact of our targeting strategy on stroma-rich tumor therapy, we evaluated the tumor-suppressive effect of TF Ab-LipDOX on KLN205 solid tumor growth. KLN205 tumor-bearing mice were intravenously injected with TF Ab-LipDOX at the indicated dosages as DOX via a tail vein; and the tumor volume after 4 treatments, with 1 given every 2 days, was measured. The results indicated that the growth of the KLN205 solid tumors was strongly suppressed by the fourth treatment with TF Ab-LipDOX and that the suppression was

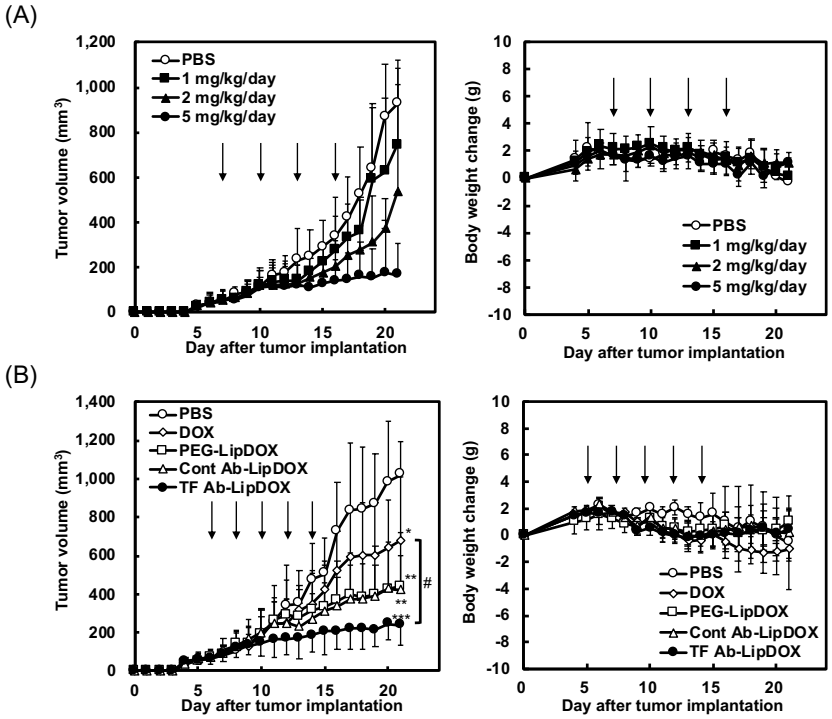

Fig. 4. Cancer chemotherapy of stroma-rich KLN205 tumors with TF Ab-LipDOX.
(A) Dosage-dependent suppression of KLN205 tumor growth by the treatment with TF Ab-LipDOX. KLN205 tumor-bearing mice were intravenously injected with PBS or TF Ab-LipDOX (1, 2 or 5 mg/kg/day as DOX dosage) at day 7, 10, 13, and 16 after the tumor implantation; and the tumor volume was monitored. Black arrows show the days of sample injection. (B) Comparison of therapeutic effect of liposomal DOX formulations on the growth of KLN205 solid tumors. KLN205 tumor-bearing mice were intravenously injected with PBS, DOX, PEG-LipDOX, Cont Ab-LipDOX or TF Ab-LipDOX (5 mg/kg/day as DOX dose) at day 6, 8, 10, 12, and 14 after tumor implantation. Body weight changes of the mice were observed in each experiment. Data are shown as the mean ± S.D. Significant differences are shown with symbols (*; $P < 0.05$, **; $P < 0.01$, ***; $P < 0.001$ vs. PBS, #; $P < 0.05$, Tukey HSD).

dependent on the DOX dosage (Fig. 4A). Then, this anti-tumor effect of TF Ab-LipDOX on the KLN205 tumor-bearing mice was compared with that of DOX, PEG-LipDOX, and Cont Ab-LipDOX. Consequently, the treatments with TF Ab-LipDOX significantly suppressed the tumor growth; and the effect was stronger than that found for the other treatment groups (Fig. 4B). As a result of this tumor-suppressive effect, the survival time of the tumor-bearing mice was prolonged

386 in the TF Ab-LipDOX-treated group: The survival-time ratio for the tumor-bearing mice treated
387 with DOX, PEG-LipDOX, Cont Ab-LipDOX, and TF Ab-LipDOX against PBS-treated group
388 was 153, 196, 181, and 220%, respectively. Furthermore, when the body weight of the tumor-
389 bearing mice was monitored as an indicator of side effects, little change was observed in any of
390 the treated groups (Fig. 4A, B). These results suggest that TF Ab-LipDOX could be useful for the
391 treatment of refractory stroma-rich tumors such as pancreatic tumors without causing severe side
392 effects.
393
394 *3.7. Targetability of TF Ab-Lip to human pancreatic tumor*
395 To demonstrate the applicability of anti-TF antibody-conjugated liposomes to stroma-
396 rich human pancreatic tumor targeting, we chose 2 human pancreatic tumor cell lines, BxPC3 and
397 Suit-2, and first compared the expression of human TF in both cell lines. The results of Western
398 blotting analysis indicated that the expression of human TF in BxPC3 cells was quite higher than
399 that in the Suit-2 cells (Fig. 5A), and so we decided to use BxPC3 tumors as a model of human
400 TF-expressing pancreatic tumors. BxPC3 solid tumor-bearing mice were prepared by
401 subcutaneously implanting the tumor cells into nude mice, and TF expression in the solid tumor
402 was confirmed. The histochemical analysis by HE staining indicated that these solid tumors had
403 a rich stromal region in the tumor tissue (Fig. 5B). Furthermore, as the results of immunostaining
404 of tumor sections, human TF was expressed in EpCAM-positive tumor cells, but not in α-SMA-
405 positive stromal cells. In contrast, mouse TF was expressed only in the α-SMA-positive stromal
406 cells (Fig. 5C). These results suggest that BxPC3 tumor-bearing mice expressed human TF in the
407 tumor cell region and mouse TF in the stromal region of the tumor tissue.
408 Next, to investigate the capability of TF Ab-Lip to target human pancreatic tumors and
409 to confirm the usefulness of the targeting approach for the treatment of BxPC3 solid tumors, we
410 prepared liposomes conjugated with anti-human TF antibody (hTF Ab-Lip), anti-mouse TF
411 antibody (mTF Ab-Lip) or both anti-hTF and mTF antibodies (mhTF Ab-Lip; Fig. S3A). When
412 the binding and uptake of hTF Ab-Lip to BxPC3 and Suit-2 tumor cells was examined, hTF Ab-
413 Lip were significantly associated with the high TF-expressing BxPC3 cells compared with the
414 association of non- targeted PEG-Lip and Cont Ab-Lip with these cells, but and associated to a
415 lesser degree with the low TF-expressing Suit-2 cells (Fig. 5D). In addition, the association of
416 hTF Ab-Lip with mouse NIH3T3 was low and similar to that of PEG-Lip or Cont Ab-Lip.
417 Furthermore, when the *in vitro* cytotoxicity of hTF Ab-LipDOX against BxPC3 cells was
418 examined, hTF Ab-LipDOX dominantly inhibited the proliferation of the tumor cells compared

with PEG-LipDOX and Cont Ab-LipDOX, with the IC_{50} values of DOX, PEG-LipDOX, Cont Ab-LipDOX, and hTF Ab-LipDOX being 0.06 μg/mL, 3.9 μg/mL, 3.0 μg/mL, and 1.5 μg/mL (Fig. 5E). These results suggest that hTF Ab-Lip enabled the targeting of human TF-expressing BxPC3 tumor cells, but not mouse TF-expressing cells. Then, we observed the intratumoral distribution of anti-TF antibody-conjugated liposomes in BxPC3 solid tumor and compared it with that obtained withPEG-Lip, Cont Ab-Lip, mTF Ab-Lip, hTF Ab-Lip, and mhTF Ab-Lip. Consequently, mhTF Ab-Lip, targeting both human TF and mouse TF, was widely distributed in the whole tumor tissue and localized in not only the α-SMA-positive mouse stromal region, but also in the other α-SMA-negative region, which was mainly composed of human BxPC3 tumor cells (Fig. 5F). On the other hand, hTF Ab-Lip accumulated in the α-SMA-negative tumor cell region, but not in the α-SMA-positive mouse stromal region; and mTF Ab-Lip showed low accumulation in the tumor tissue, but a portion of them was localized in the α-SMA-positive mouse stromal region. Finally, we carried out the therapeutic experiment using BxPC3 tumor-bearing mice and examined anti-pancreatic tumor effect of mhTF Ab-LipDOX enables to target both mouse TF-expressing tumor stromal cells and human TF-expressing tumor cells on mouse stroma-rich human tumor. The result showed that mhTF Ab-LipDOX significantly suppressed the growth of BxPC3 tumor and the tumor-suppressive effect was highest in the treated groups (Fig. 5G). These results strongly suggest that TF targeting by anti-TF antibody-conjugated liposomes can provide drug delivery to TF-expressing stroma-rich tumors and that TF-targeting drug delivery strategy is useful for the treatment of human stroma-rich pancreatic tumors.

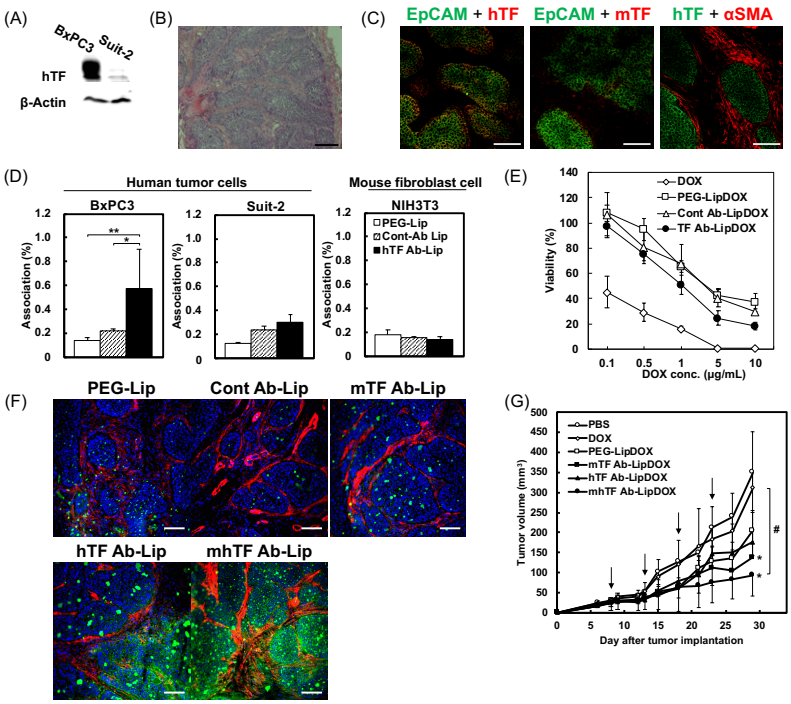

Fig. 5. Human pancreatic tumor targeting by TF-targetable liposomes

(A) TF expression in human pancreatic tumor cells. The expression levels of human TF and β-actin in human pancreatic BxPC3 or Suit-2 cells were examined by Western blotting. (B) Histological analysis of BxPC3 solid tumors. Paraffin sections of BxPC3 solid tumors were prepared and stained with H&E. Scale bars represent 200 μm. (C) Expression of TF in BxPC3 solid tumors. Frozen sections of the BxPC3 solid tumor were prepared and fluorescently stained for human TF, mouse TF, α-SMA, or EpCAM to visualize the stromal cells or tumor cells, respectively. Nuclei were stained with DAPI. Scale bars: 100 μm. (D) Targeting of hTF Ab-Lip to hTF-expressing tumor cells. BxPC3 cells, SUIT-2 cells or NIH3T3 cells were incubated with $DiIC_{18}$-labeled PEG-Lip, Cont Ab-Lip or hTF Ab-Lip for 24 h at 37ºC. After the cells had been washed with PBS, the amount of liposome association with the cells was determined by measuring the fluorescence intensity. Data are shown as the mean of uptake (%) and the S.D. Significant differences are shown with asterisk (*: $P < 0.05$, **: $P < 0.01$, Tukey HSD). (E) BxPC3 cells were incubated with DOX, PEG-LipDOX, Cont Ab-LipDOX or TF Ab-LipDOX at 37ºC for 12 h. After a washing of the cells with PBS, the cells were cultured in fresh medium for 48 h. Then, cell viability was determined by performing a WST-8 assay. Data are shown as the mean of viability (%) and S.D. (F) Intratumoral distribution of TF Ab-Lip in BxPC3 solid tumors. $DiOC_{18}$ (green)-labeled PEG-Lip, Cont Ab-Lip, anti-mouse TF antibody-conjugated liposomes (mTF Ab-Lip), anti-human TF antibody-conjugated liposomes (hTF Ab-Lip), or both anti-mouse and anti-human TF antibody-conjugated liposomes (mhTF Ab-Lip) were intravenously injected into BxPC3 tumor-bearing mice. Twenty-four hours after the injection, frozen sections of the tumor tissue were prepared. Immunofluorescence staining of mouse α-SMA (red) was performed to visualize tumor-associated stromal cells. Nuclei were stained by DAPI (blue). The fluorescence images of the sections were observed by using a confocal laser-scanning microscope. Scale bars represent 100 μm. (G) Suppressive effect of DOX-encapsulated TF Ab-Lip on BxPC3 solid tumor growth. BxPC3 tumor-bearing mice were intravenously injected with PBS, DOX, PEG-LipDOX, DOX-encapsulated mTF Ab-Lip (mTF Ab-LipDOX), hTF Ab-Lip (hTF Ab-LipDOX) or mhTF Ab-Lip (mhTF Ab-LipDOX) (5 mg/kg/day as DOX dose) via a tail vein at day 8, 13, 18, and 23 after tumor implantation. Data are shown as the mean ± S.D. Significant differences are shown (*; $P < 0.05$ vs. PBS, #; $P < 0.05$, Tukey HSD).

4. Discussion

Formation of tumor stroma is regulated by certain cytokines, and especially TGF-β is a representative of such molecules [2]: TGF-β is secreted from tumor cells and tumor-associated macrophages and stimulates fibroblast cells, which in turn then express certain molecules such as α-SMA. These activated fibroblasts, referred to as tumor-associated fibroblasts, begin to proliferate to form a thick stroma composed of collagen molecules, resulting in a collagen network between tumor cells and the stroma [13]. This microenvironment-formation event is very important for both tumor cell growth and acquisition of drug resistance by the tumor. In fact, the pancreatic tumor, a representative stroma-rich tumor, is a malignancy that acquires drug resistance due to poor delivery of anti-cancer drugs to the tumor tissue [14]. To improve the therapeutic effect of drugs on pancreatic tumors, several approaches using DDS medicines have been developed [5, 15]. Among them, our collaborator Matsumura has advocated a novel cancer therapeutic concept, called cancer stromal targeting (CAST), which is a stroma-targeting strategy that enables a drug concentration to be enhanced in stroma-rich tumor tissues, thereby eradicating the tumor cells indirectly [16]. Actually, they developed an anti-insoluble fibrin antibody as a targeting probe for tumor stromal cells [17] and demonstrated the potential usages of the CAST approach for pancreatic cancer therapy [18] and diagnosis [19]. TF is another suitable candidate molecule for CAST, since TF is normally expressed in the extravascular stroma of normal tissues [20]. Additionally, it has been reported that stimulation of fibroblast cells with TGF-β increases the expression of TF in the tumor stroma [10]. Besides, TF expression is enhanced in certain kinds of tumor cells, because the binary complex of TF and factor VII on the membrane of tumor cells promotes tumor cell growth, migration, survival, and angiogenic stimulation via activation of the protease-activated receptor (PAR)-2 [21, 22]. Our presently presented strategy for the treatment of stroma-rich tumors is to enhance liposome delivery via TF targeting in both tumor cells and tumor stromal cells. In the experiments using cultured cell lines, we found that TF was highly expressed in KLN205 and B16 tumor cells, and non-tumorous NIH3T3 fibroblast cells, but poorly expressed in Colon26 tumor cells and 2H-11 endothelial cells (Fig. 1A). Reflecting this result, TF expression was obviously observed in the KLN205 solid tumor, but was quite low in Colon26 solid tumor (Fig. 1B). Furthermore, the TF expression was observed not only in the α-SMA-negative, but also in the α-SMA-positive, region and distributed throughout the KLN205 tumor tissue (Fig. 1D). We also found that the expression of α-SMA in the KLN205 tumor was evident in the non-tumorous EpCAM-negative region around CD31-positive blood vessels (Fig. S1A), indicating that the KLN205 solid tumor had a rich stroma. In

contrast, the expression of α-SMA was colocalized with CD31-positive blood vessels in the low TF-expressing Colon26 solid tumor (Fig. S1B), indicating that the Colon26 solid tumor consisted mostly of the tumor cells and that α-SMA was expressed in the vascular smooth muscle cells. These data suggest that TF was expressed in not only tumor cells, but also tumor stromal cells in the KLN205 tumor, making TF a promising and suitable target molecule for drug delivery to stroma-rich tumors.

To achieve the active targeting of liposomes via the TF molecule, we prepared PEG-modified liposomes conjugated with anti-TF antibody on the tip of the PEG chain as a drug carrier; since an antibody has the potential to strongly and specifically recognize a target molecule. PEG-modified liposomes pre-sized to less than 200 nm in diameter passively accumulate in angiogenic vessel-rich solid tumors after systemic injection via the enhanced permeability and retention (EPR) effect, which provides a major mechanism of tumor targeting by drug nanocarriers [23]. Our previous study demonstrated that modification of angiogenic vessel-targetable peptide on the tip of PEG chains of PEG-modified liposomes is suitable for recognition of target molecules [24], because long-time circulation of liposomes in the bloodstream by PEG modification enhances the chance for interaction between the targeting probe with the targeted molecule on the surface of angiogenic endothelial cells as well as accumulation in the tumor by the EPR effect [25]. Particle sizes of prepared TF Ab-Lip and TF Ab-LipDOX were less than 150 nm and quite similar to those of PEG-Lip, Cont Ab-Lip, PEG-LipDOX, and Cont Ab-LipDOX, suggesting that they could be expected to not only demonstrate the EPR effect but also actively target the TF-expressing tumors. Actually, TF-Ab-Lip was significantly taken up into high TF-expressing tumor cells and fibroblast cells, but not into low-TF-expressing tumor cells and endothelial cells (Fig. 2B). Furthermore, high accumulation of TF-Ab-Lip in the KLN205 solid tumor occurred after the systemic injection into tumor-bearing mice following long-time circulation in the bloodstream, as was also observed with PEG-Lip (Fig. 3A). Notably, TF Ab-Lip was distributed throughout the tumor tissue and retained in the tissue after the blood had been washed out of the tumor by perfusion with PBS; whereas almost all of the PEG-Lip and Cont Ab-Lip in the tumor tissue were washed out by the perfusion (Fig. 3C). Moreover, TF Ab-Lip accumulated in both the α-SMA-positive stromal region as well as in the tumor cell region (Fig. 3D). These lines of evidence proved the targeting capability of TF Ab-Lip and the improvement of drug delivery to stroma-rich tumors following cellular uptake of the liposomes. In fact, we demonstrated the potent therapeutic effect of TF Ab-LipDOX on stroma-rich KLN205 tumor growth (Fig. 4).

To demonstrate the targeting capability of TF-targeted liposomes in detail, we carried out unique experiments using human pancreatic BxPC3 tumor-bearing mice. The BxPC3 tumor contained rich stroma; and immunostaining of tumor sections showed that the expression of human TF in the EpCAM-positive tumor cell region but not in the α-SMA-positive stromal region, whereas mouse TF was expressed in the α-SMA-positive stromal one (Fig. 5B, C). Then, human TF-targetable liposomes were prepared by modification of PEG-conjugated liposomes with anti-human TF antibody (Fig. S3). hTF Ab-Lip were significantly taken up into BxPC3 cells (high hTF-expressing), but not into Suit-2 (low hTF-expressing) or NIH3T3 cells, suggesting that hTF Ab-Lip could target only human TF-expressing tumor cells (Fig. 5D). To demonstrate the utility of our targeting strategy for effective drug delivery to the human pancreatic tumors and prove our present research concept, we analyzed the intratumoral distribution of both mouse TF- and human TF-targetable liposomes after systemic injection into BxPC3 tumor-bearing mice. Consequently, mhTF Ab-Lip were located at both mouse TF-expressing stromal region and human TF-expressing tumor cell region in the tumor tissue, suggesting that the TF-targetable liposomes can be applicable for the treatment of stroma-rich human pancreatic tumors. Kataoka and his colleagues previously demonstrated the potential usage of anti-human TF antibody to deliver micellar nanoparticles loaded with epirubicin or siRNA to human TF-expressing BxPC3 tumors for human pancreatic cancer therapy [26, 27]. Also, our collaborator Matsumura *et al.* used antibody-drug conjugate (ADC) drug for pancreatic tumor imaging [28], since the anti-human TF antibody enables recognition of human TF molecules on the pancreatic tumor cells. Our targeting DDS strategy is the combination of conventional tumor cell targeting with CAST via the TF molecule: Liposomes accumulated in tumor tissue by the EPR effect can recognize both TF-expressing tumor cells and TF-expressing stromal cells via anti-TF antibody and are taken up into both cells. The importance of stromal targeting in the treatment of stroma-rich tumors has already been reported by some researchers. For example, Huang *et al.* recently demonstrated that systemic injection of quercetin phosphate nanoparticles reduced the number of α-SMA-positive fibroblasts via the inhibition of Wnt16 expression and showed their suppressive effect on the growth of stroma-rich bladder tumor in combination with cisplatin nanoparticle treatment [29, 30]. Also, Zhou *et al.* focused on sonic hedgehog (SHH) signaling, which is strongly involved in the interaction between pancreatic tumor cells and activated fibroblast cells, and demonstrated that synergistic combination of an SHH inhibitor, GDC-0449, with PEGylated liposomal DOX exhibited potent antitumor efficacy toward BxPC3 tumor growth [31]. These lines of evidence strongly support the validity of our targeting DDS strategy with anti-TF antibody-conjugated

liposomes for the treatment of pancreatic tumors. Actually, we demonstrated the importance of both targeting of tumor and tumor stromal cells in the treatment of stroma-rich pancreatic tumors for the first time by performing the therapeutic experiment using BxPC3 tumor model (Fig. 5G): Only mhTF Ab-LipDOX could target and damage both mouse TF-expressing stroma cells and human TF-expressing pancreatic BxPC3 cells. In current clinical situation of cancer chemotherapy, application of targeted delivery system with ligand-conjugated drug carriers has not yet been mainstream, despite the defined therapeutic outcomes are being achieved in basic researches with animal models. It is no doubt that the EPR effect is a principle concept of macromolecule delivery to solid tumors, however tumor microenvironment varies according to the type of tumors and the existence of thick stroma in tumor tissue is one of the reasons why the DDS drugs failed to produce the EPR effect and to reach tumor cells. Our targeted strategy with anti-TF antibody-modified liposomes could overcome the poor drug delivery of macromolecules to stroma-rich tumors by targeting both tumor cells and stromal cells and breaking the barrier of stroma.

5. Conclusion

In the present study, we demonstrated that TF Ab-Lip improved the anti-cancer drug delivery to stroma-rich tumors by active targeting of both tumor cells and tumor stromal cells via the strong interaction of liposome-surface anti-TF antibody with cell-surface TF molecules (Fig. 6). We believe that this targeting DDS strategy would be applicable for the treatment of stroma-rich malignant tumors including pancreatic tumors.

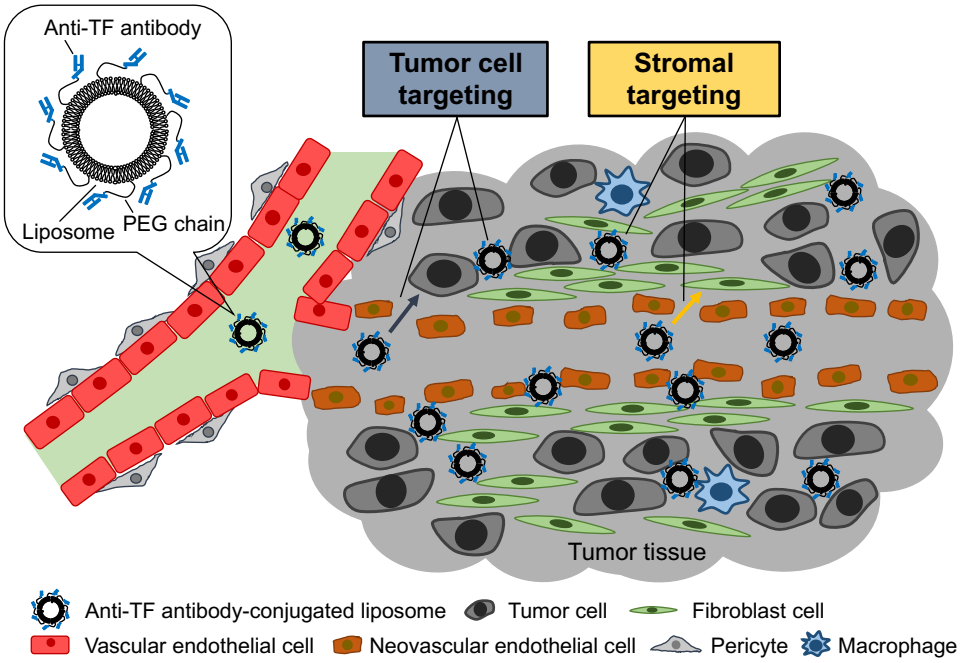

Fig. 6. Tumor cell and tumor stromal targeting with anti-TF antibody-modified liposomes
Stroma-rich tumors such as pancreatic tumors are malignant and acquire their drug resistance due to poor delivery of anti-cancer drugs to the tumor tissue due to the fact that the thick stroma region surrounding the tumor cells prevents drugs from gaining access to the tumor cells. The present targeting DDS strategy can solve this problem by targeting not only tumor cells but also the tumor stroma including activated fibroblast cells with a liposomal probe targeting both tumor and stromal cells. As a result, potent cancer therapy of these stroma-rich tumors can be achieved. TF is a suitable molecule for immuno-targeting both tumor and stromal cells, since TF is highly expressed in both kinds of cells. Thus, anti-TF antibody-conjugated liposome is an applicable drug carrier to treat stroma-rich tumors.

Acknowledgements

This research was supported in part by National Cancer Center Research and Development Fund (29-A-9 to Y.M.) and University of Shizuoka.

Conflict of interest

Yasuhiro Matsumura is a Co-founder and a stock holder of RIN Institute Inc. The other authors declare that there are no conflicts of interest.

References

[1] P.C. Benias, R.G. Wells, B. Sackey-Aboagye, H. Klavan, J. Reidy, D. Buonocore, M. Miranda, S. Kornacki, M. Wayne, D.L. Carr-Locke, N.D. Theise, Structure and distribution of an unrecognized interstitium in human tissues, Sci. Rep. 8 (2018) 4947.

[2] P. Papageorgis, T. Stylianopoulos, Role of tgfbeta in regulation of the tumor microenvironment and drug delivery (review), Int. J. Oncol. 46 (2015) 933-943.

[3] L. Caja, F. Dituri, S. Mancarella, D. Caballero-Diaz, A. Moustakas, G. Giannelli, I. Fabregat, Tgf-beta and the tissue microenvironment: Relevance in fibrosis and cancer, Int. J. Mol. Sci. 19 (2018) 1294.

[4] D. von Ahrens, T.D. Bhagat, D. Nagrath, A. Maitra, A. Verma, The role of stromal cancer-associated fibroblasts in pancreatic cancer, J. Hematol. Oncol. 10 (2017) 76.

[5] P.P. Adiseshaiah, R.M. Crist, S.S. Hook, S.E. McNeil, Nanomedicine strategies to overcome the pathophysiological barriers of pancreatic cancer, Nat. Rev. Clin. Oncol. 13 (2016) 750-765.

[6] H.F. Dvorak, Tumors: Wounds that do not heal. Similarities between tumor stroma generation and wound healing, N. Engl. J. Med. 315 (1986) 1650-1659.

[7] P.D. Stein, A. Beemath, F.A. Meyers, E. Skaf, J. Sanchez, R.E. Olson, Incidence of venous thromboembolism in patients hospitalized with cancer, Am. J. Med. 119 (2006) 60-68.

[8] Y. Matsumura, M. Kimura, T. Yamamoto, H. Maeda, Involvement of the kinin-generating cascade in enhanced vascular permeability in tumor tissue, Jpn. J. Cancer Res. 79 (1988) 1327-1334.

[9] H.F. Dvorak, Vascular permeability factor/vascular endothelial growth factor: A critical cytokine in tumor angiogenesis and a potential target for diagnosis and therapy, J. Clin. Oncol. 20 (2002) 4368-4380.

[10] J.A. Vrana, M.T. Stang, J.P. Grande, M.J. Getz, Expression of tissue factor in tumor stroma correlates with progression to invasive human breast cancer: Paracrine regulation by carcinoma cell-derived members of the transforming growth factor beta family, Cancer Res. 56 (1996) 5063-5070.

[11] Y. Saito, Y. Hashimoto, J. Kuroda, M. Yasunaga, Y. Koga, A. Takahashi, Y. Matsumura, The inhibition of pancreatic cancer invasion-metastasis cascade in both cellular signal and blood coagulation cascade of tissue factor by its neutralisation antibody, Eur. J. Cancer 47 (2011) 2230-2239.

[12] T.M. Allen, P.R. Cullis, Liposomal drug delivery systems: From concept to clinical applications, Adv Drug Deliv Rev 65 (2013) 36-48.

[13] L. Narunsky, R. Oren, F. Bochner, M. Neeman, Imaging aspects of the tumor stroma with therapeutic implications, Pharmacol. Ther. 141 (2014) 192-208.

[14] B. Uzunparmak, I.H. Sahin, Pancreatic cancer microenvironment: A current dilemma, Clin Transl Med 8 (2019) 2.

[15] L. Miao, L. Huang, Exploring the tumor microenvironment with nanoparticles, Cancer Treat.

612 Res. 166 (2015) 193-226.
613 [16] Y. Matsumura, Cancer stromal targeting (cast) therapy, Adv Drug Deliv Rev 64 (2012) 710-
614 719.
615 [17] Y. Hisada, M. Yasunaga, S. Hanaoka, S. Saijou, T. Sugino, A. Tsuji, T. Saga, K. Tsumoto, S.
616 Manabe, J. Kuroda, J. Kuratsu, Y. Matsumura, Discovery of an uncovered region in fibrin
617 clots and its clinical significance, Sci. Rep. 3 (2013) 2604.
618 [18] M. Yasunaga, S. Manabe, A. Tsuji, M. Furuta, K. Ogata, Y. Koga, T. Saga, Y. Matsumura,
619 Development of antibody-drug conjugates using dds and molecular imaging, Bioengineering
620 (Basel) 4 (2017) 78.
621 [19] H. Fuchigami, S. Manabe, M. Yasunaga, Y. Matsumura, Chemotherapy payload of anti-
622 insoluble fibrin antibody-drug conjugate is released specifically upon binding to fibrin, Sci.
623 Rep. 8 (2018) 14211.
624 [20] H.H. Versteeg, M.P. Peppelenbosch, C.A. Spek, The pleiotropic effects of tissue factor: A
625 possible role for factor viia-induced intracellular signalling?, Thromb. Haemost. 86 (2001)
626 1353-1359.
627 [21] E. Camerer, W. Huang, S.R. Coughlin, Tissue factor- and factor x-dependent activation of
628 protease-activated receptor 2 by factor viia, Proc. Natl. Acad. Sci. U. S. A. 97 (2000) 5255-
629 5260.
630 [22] M.Z. Wojtukiewicz, D. Hempel, E. Sierko, S.C. Tucker, K.V. Honn, Protease-activated
631 receptors (pars)--biology and role in cancer invasion and metastasis, Cancer Metastasis Rev.
632 34 (2015) 775-796.
633 [23] Y. Matsumura, H. Maeda, A new concept for macromolecular therapeutics in cancer
634 chemotherapy: Mechanism of tumoritropic accumulation of proteins and the antitumor agent
635 smancs, Cancer Res. 46 (1986) 6387-6392.
636 [24] T. Sugiyama, T. Asai, Y.M. Nedachi, Y. Katanasaka, K. Shimizu, N. Maeda, N. Oku,
637 Enhanced active targeting via cooperative binding of ligands on liposomes to target receptors,
638 PLoS One 8 (2013) e67550.
639 [25] N. Maeda, Y. Takeuchi, M. Takada, Y. Sadzuka, Y. Namba, N. Oku, Anti-neovascular therapy
640 by use of tumor neovasculature-targeted long-circulating liposome, J. Control. Release 100
641 (2004) 41-52.
642 [26] A. Sugaya, I. Hyodo, Y. Koga, Y. Yamamoto, H. Takashima, R. Sato, R. Tsumura, F. Furuya,
643 M. Yasunaga, M. Harada, R. Tanaka, Y. Matsumura, Utility of epirubicin-incorporating
644 micelles tagged with anti-tissue factor antibody clone with no anticoagulant effect, Cancer

Sci. 107 (2016) 335-340.
[27] H.S. Min, H.J. Kim, J. Ahn, M. Naito, K. Hayashi, K. Toh, B.S. Kim, Y. Matsumura, I.C. Kwon, K. Miyata, K. Kataoka, Tuned density of anti-tissue factor antibody fragment onto sirna-loaded polyion complex micelles for optimizing targetability into pancreatic cancer cells, Biomacromolecules 19 (2018) 2320-2329.
[28] Y. Koga, S. Manabe, Y. Aihara, R. Sato, R. Tsumura, H. Iwafuji, F. Furuya, H. Fuchigami, Y. Fujiwara, Y. Hisada, Y. Yamamoto, M. Yasunaga, Y. Matsumura, Antitumor effect of antitissue factor antibody-mmae conjugate in human pancreatic tumor xenografts, Int. J. Cancer 137 (2015) 1457-1466.
[29] L. Miao, Y. Wang, C.M. Lin, Y. Xiong, N. Chen, L. Zhang, W.Y. Kim, L. Huang, Nanoparticle modulation of the tumor microenvironment enhances therapeutic efficacy of cisplatin, J. Control. Release 217 (2015) 27-41.
[30] K. Hu, L. Miao, T.J. Goodwin, J. Li, Q. Liu, L. Huang, Quercetin remodels the tumor microenvironment to improve the permeation, retention, and antitumor effects of nanoparticles, ACS Nano 11 (2017) 4916-4925.
[31] Q. Zhou, Y. Zhou, X. Liu, Y. Shen, Gdc-0449 improves the antitumor activity of nano-doxorubicin in pancreatic cancer in a fibroblast-enriched microenvironment, Sci. Rep. 7 (2017) 13379.

Supplementary data

Table S1. Formulation characteristics of TF-modified liposomes

	Particle Size (nm)	PDI	ζ-Potential (mV)	Antibody (μg/mL)
PEG-modified liposome (PEG-Lip)	133 ± 16	0.15 ± 0.06	-3.0 ± 2.9	Not applicable
Control Ab-modified liposome (Cont Ab-Lip)	141 ± 15	0.17 ± 0.07	-8.3 ± 1.2	400 ± 35
Anti-mTF Ab-modified liposome (TF Ab-Lip)	130 ± 6	0.16 ± 0.08	-8.8 ± 1.4	309 ± 24

	Particle size (nm)	PDI	ζ-Potential (mV)	DOX (μg/mL)
PEG-modified liposomal DOX (PEG-LipDOX)	132 ± 18	0.12 ± 0.06	-2.3 ± 1.6	430 ± 44
Control Ab-modified liposomal DOX (Cont Ab-LipDOX)	145 ± 25	0.15 ± 0.08	- 6.2 ± 1.3	425 ± 62
Anti-mTF Ab-modified liposomal DOX (TF Ab-LipDOX)	141 ± 12	0.12 ± 0.08	-7.3 ± 1.9	419 ± 60

The liposome solution was diluted with PBS, and the particle size and ζ-potential were measured by use of a Zetasizer Nano system. Ab: antibody; DOX: doxorubicin; PDI: polydispersity index.

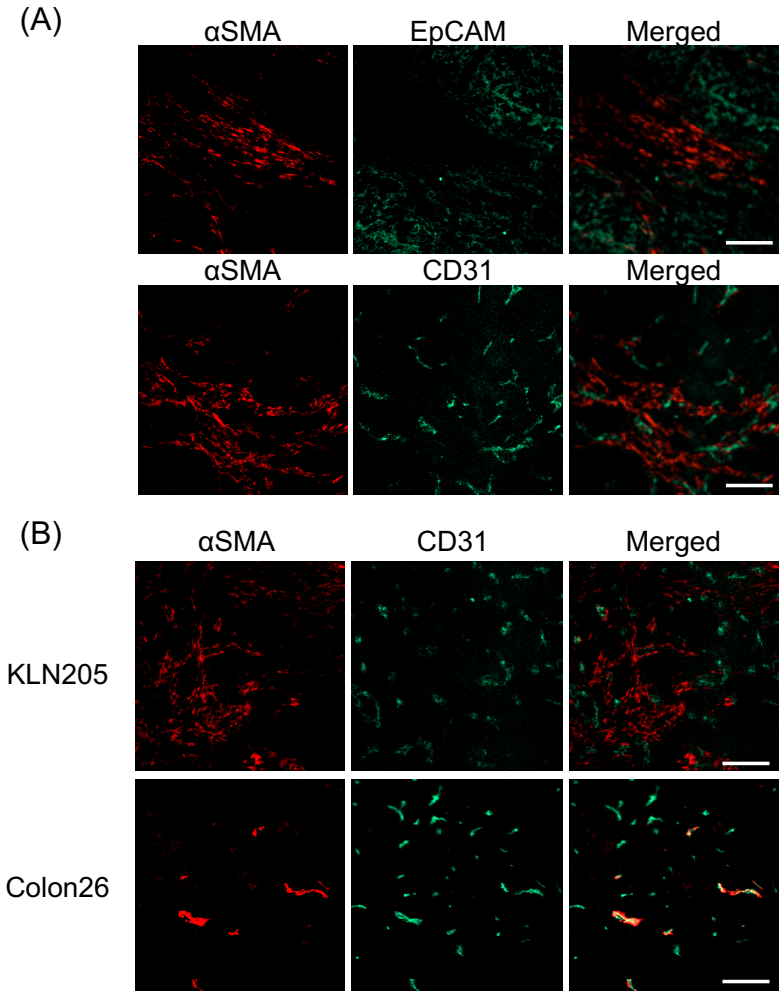

Fig. S1. Observation of tumor microenvironment of solid tumors.

KLN205 cells (5 x 10^6 cells/mouse) or Colon26 NL-17 (Colon26) cells (1 x 10^6 cells/mouse) were implanted subcutaneously into DBA/2 or BALB/c mice, respectively to prepare tumor-bearing mice. Then, the solid tumors were collected, and the frozen sections of the tumors were prepared. (A) Immunofluorescence staining of αSMA (red), EpCAM (green) or CD31 (green) was performed to visualize tumor-associated stromal cells, tumor cells or blood vessels, respectively, in the KLN205 tumor. (B) For comparison of the tumor microenvironment between KLN205 and C26NL17 solid tumors, immunofluorescence staining of αSMA (red) and CD31 (green) was performed. Fluorescent images of the tumor sections were observed by using a confocal laser-scanning microscope. Scale bars represent 100 μm.

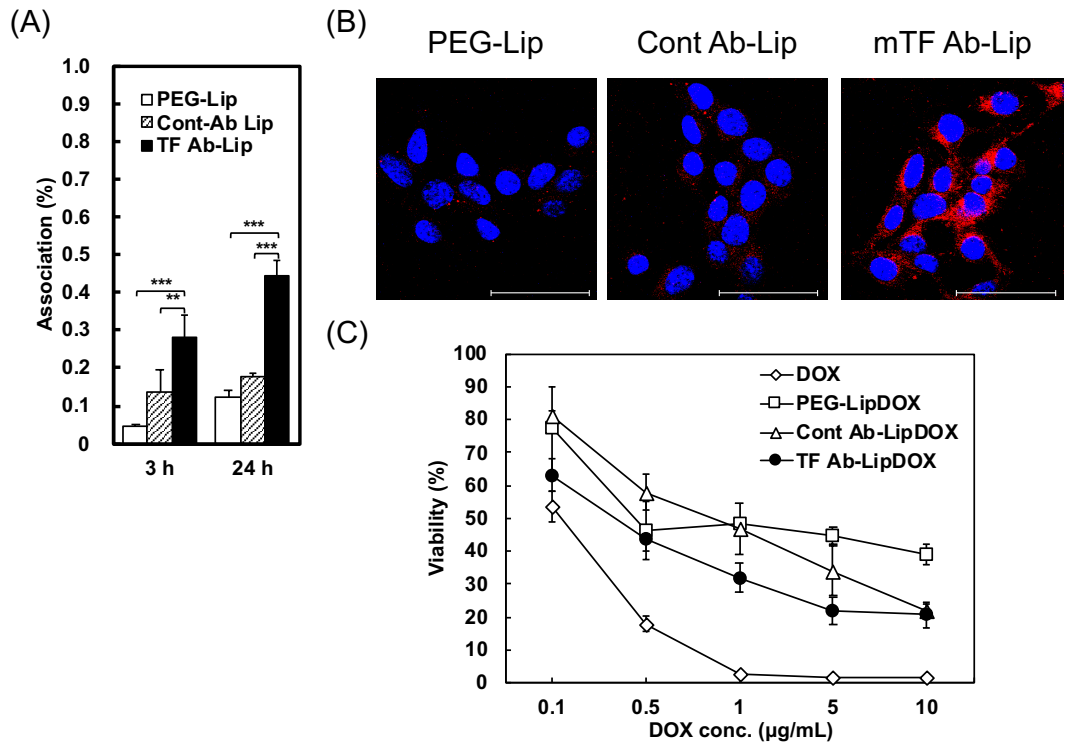

Fig. S2. Targetability of TF Ab-Lip to TF-expressing B16F10 tumor cells.

(A) Quantitative analysis of liposome association with B16F10 cells. Mouse melanoma B16F10 cells were incubated with $DiIC_{18}$-labeled PEG-Lip, Cont Ab-Lip or mTF Ab-Lip for 3 or 24 h at 37ºC. After the cells had been washed with PBS, they were solubilized with 0.1% SDS solution. The amount of liposomes associated with the cells was determined by measuring the fluorescence intensity. Data are shown as the mean of uptake (%) and the S.D. Significant differences are shown with asterisks (**: $P < 0.01$, ***: $P < 0.001$). (B) Intracellular uptake of TF Ab-Lip into B16F10 cells. After incubation of the cells with $DiIC_{18}$-labeled PEG-Lip, Cont Ab-Lip or mTF Ab-Lip for 3 h, the cells were fixed with 4% paraformaldehyde, after which the nuclei were stained with DAPI. Intracellular uptake of the liposomes was observed by confocal laser scanning microscopy. Scale bars represent 50 μm. (C) B16F10 cells were incubated with doxorubicin-encapsulated PEG-Lip (PEG-LipDOX, □), Cont Ab-Lip (Cont Ab-LipDox, △) or TF Ab-Lip (TF Ab-DOX, ●) at 37 ºC for 12 h. After washing of the cells with PBS, the cells were cultured in fresh medium for 48 h. Then cell viability was determined by use of the WST-8 assay. Data are shown as the mean of viability (%) and S.D. IC_{50} values of PEG-LipDOX, Cont Ab-LipDOX, and TF Ab-LipDOX were 1.2, 1.0, and 0.28 μg/mL as DOX concentration, respectively.

(A)

	Particle size (nm)	PDI	ζ-Potential (mV)
Anti-hTF Ab-modified liposome (hTF Ab-Lip)	148 ± 2.0	0.13 ± 0.02	-8.8 ± 2.3
Anti-mTF and -hTF Abs-modified liposome (mhTF Ab-Lip)	151 ± 0.3	0.10 ± 0.03	-9.0 ± 2.4

(B)

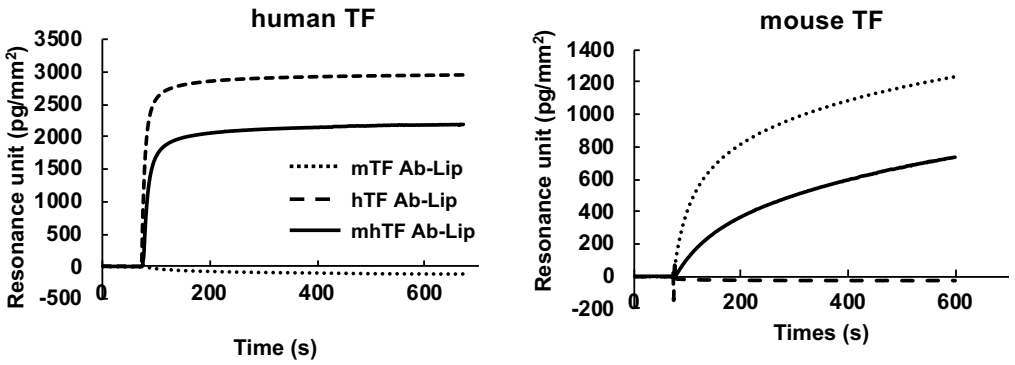

Fig. S3. Formulation characteristics of hTF Ab-Lip and mhTF Ab-Lip.

(A) Physicochemical properties of hTF Ab-Lip and mhTF Ab-Lip. The liposome solution was diluted with PBS, and the particle size and ζ-potential were measured by using the Zetasizer Nano system. Ab: antibody; PDI: polydispersity index. (B) Capabilities of hTF Ab-Lip and mhTF Ab-Lip to bind to recombinant TFs. Mouse TF or human TF was immobilized on the sensor chip CM5. mTF Ab-Lip, hTF Ab-Lip or mhTF Ab-Lip were applied on each sensor chip; and the interaction was analyzed with the Biacore system.